SYVN1 Promotes STAT3 Protein Ubiquitination and Exerts Antiangiogenesis Effects in Retinopathy of Prematurity Development

Shimei Chen,[1] Jian Zhang,[1] Dandan Sun,[1] Yidong Wu,[1] Junwei Fang,[1] Xiaoling Wan,[1] Shenping Li,[1] Shuchang Zhang,[1] Qing Gu,[1] Qing Shao,[2] Jun Dong,[2] Xun Xu,[1] Fang Wei,[1] and Qiao Sun[1,2]

[1]Department of Ophthalmology, Shanghai General Hospital, Shanghai Jiao Tong University School of Medicine, Shanghai Key Laboratory of Ocular Fundus Diseases, Shanghai Engineering Center for Visual Science and Photomedicine, National Clinical Research Center for Eye Diseases, Shanghai Engineering Center for Precise Diagnosis and Treatment of Eye Diseases, Shanghai, China
[2]Department of Ophthalmology, Shanghai Aier Eye Hospital, Xuhui District, Shanghai Aier Eye Institute, Shanghai, China

Correspondence: Qiao Sun and Fang Wei, Department of Ophthalmology, Shanghai General Hospital, Shanghai Jiao Tong University School of Medicine, Shanghai Key Laboratory of Ocular Fundus Diseases, Shanghai Engineering Center for Visual Science and Photomedicine, National Clinical Research Center for Eye Diseases, Shanghai Engineering Center for Precise Diagnosis and Treatment of Eye Diseases, Shanghai 200080, China;
verasun0305@aliyun.com or weifang73@hotmail.com.

SC and JZ contributed equally to this work.

Received: March 13, 2023
Accepted: July 17, 2023
Published: August 4, 2023

Citation: Chen S, Zhang J, Sun D, et al. SYVN1 promotes STAT3 protein ubiquitination and exerts antiangiogenesis effects in retinopathy of prematurity development. *Invest Ophthalmol Vis Sci.* 2023;64(11):8. https://doi.org/10.1167/iovs.64.11.8

Purpose. SYVN1, a gene involved in endoplasmic reticulum-associated degradation, has been found to exert a protective effect by inhibiting inflammation in retinopathy. This study aimed to clarify whether SYVN1 is involved in the pathogenesis of retinopathy of prematurity (ROP) and its potential as a candidate for target therapy.

Methods. Human retinal microvascular endothelial cells (hRMECs) and a mouse model of oxygen-induced retinopathy (OIR) were used to reveal the retinopathy development-associated protein expression and molecular mechanism. An adenovirus overexpressing SYVN1 or vehicle control was injected intravitreally at postnatal day 12 (P12), and the neovascular lesions were evaluated in retinal flatmounts with immunofluorescence staining, and hematoxylin and eosin staining at P17. Visual function was assessed by using electroretinogram (ERG).

Results. Endogenous SYVN1 expression dramatically decreased in hRMECs under hypoxia and in ROP mouse retinas. SYVN1 regulated the signal transducer and activator of transcription 3 (STAT3)/vascular endothelial growth factor (VEGF) axis. SYVN1 overexpression promoted ubiquitination and degradation of STAT3, decreased the levels of phospho-STAT3, secretion of VEGF, and formation of neovascularization in hRMECs, which could be rescued by STAT3 activator treatment. In addition, SYVN1 overexpression prevented neovascularization and extended physiologic retinal vascular development in the retinal tissues of OIR mice without affecting retinal function.

Conclusions. SYVN1 has a protective effect against OIR, and the molecular mechanisms are partly through SYVN1-mediated ubiquitination of STAT3 and the subsequent downregulation of VEGF. These findings strongly support our assumption that SYVN1 confers ROP resistance and may be a potentially novel pharmaceutical target against proliferative retinopathy.

Keywords: retinopathy of prematurity, SYVN1, ubiquitination, STAT3, angiogenesis

As a leading cause of childhood blindness,[1] retinopathy of prematurity (ROP) in the pediatric population is associated with abnormal blood vessel networks. Although with an increasing survival rate,[2,3] the prevalence of ROP is shown to be in an upward trend.[4,5] ROP imposes a heavy burden on families and society as the disease progresses rapidly, and the time window left for effective treatment is very narrow.[6] A common consequence of this disease is disorganized angiogenesis, which can eventually lead to fibrotic scarring, retinal detachment, and blindness.[7–9] In current clinical practice, both cryotherapy and laser treatment have severe side effects.[10,11] Despite considerable progress in anti-vascular endothelial growth factor (VEGF) therapy,[12] low serum VEGF levels may persist for up to 8 weeks after intravitreal administration and may interfere with neuronal survival in the retina.[13–15] Anti-VEGF therapy also has the adverse consequences of inhibiting physiological revascularization.[16,17] Therefore, it is encouraged to find new alternative therapies that could block excessive angiogenesis and restore physiological vasculature simultaneously to aid global efforts against the ROP epidemic.

We previously documented that activation of the Janus kinase 2-signal transducer and activator of transcription 3 (JAK2/STAT3) signaling pathway plays a central role during the proliferative stages in oxygen-induced retinopathy (OIR) mice.[18] As an important risk factor for ROP, STAT3 can

modulate retinal neovascularization (RNV) by activating VEGF, generating RNV in OIR models.[19–21] Previous studies have reported that the inhibition of STAT3 could preclude intravitreal neovascularization (IVNV) but did not affect normal retinal revascularization in an OIR rat model, indicating its unique role in the pathophysiology of ROP.[22]

Interestingly, we used an online prediction database, UbiBrowser (http://ubibrowser.bio-it.cn/ubibrowser_v3/), to unexpectedly determine that synoviolin (SYVN1) may interact with STAT3. SYVN1, an E3 ubiquitin ligase, performs essential functions in recognizing misfolded and nonfunctional proteins in the endoplasmic reticulum (ER)-associated degradation (ERAD). This protein uses the ubiquitin-proteasome system to suppress the unfolded protein response (UPR), which is important in pathological processes, such as chronic inflammation, cellular immune homeostasis, and apoptosis.[23–25] Recently, evidence has shown that UPR plays a contributing role in regulating pro-angiogenic factors and inflammatory events in retinal vascular development, which further exacerbates diabetic retinopathy (DR), ROP, and age-related macular degeneration.[26–28] However, the mechanisms of UPR in the regulation of retinal angiogenesis have yet to be elucidated. Consistently, there is growing evidence that ER stress-associated protein SYVN1 offers protection against retinal disease.[29–32] For example, Yang et al. elucidated that *SYVN1* exerts a protective effect in the development and progression of DR.[31] Zhang et al. also confirmed that *SYVN1* relieves DR by inhibiting inflammatory cytokines secreted by Müller cells by reducing NLRP3.[32] Together, these observations suggest that SYVN1 may be an alternative to slow down the progression of proliferative retinopathies. However, it remains unknown whether the expression of SYVN1 affects the pathobiology of retinal angiogenesis and physiological revascularization in ROP. Therefore, the exploration and evaluation of the effects of SYVN1 on ROP have attracted great interest.

In the current study, we first reported a decreased SYVN1 protein expression in hypoxia-treated human retinal microvascular endothelial cells (hRMECs) and OIR mouse retina, implying the role of SYVN1 in regulating the retinal vasculature. Moreover, we demonstrated, for the first time, that SYVN1 mediates STAT3 ubiquitination and reduces VEGF secretion. These findings suggest that the SYVN1/STAT3 regulatory network inhibits neovascularization during ROP treatment.

Methods

Adenoviruses and hRMEC Culture

Human adenovirus (Ad) Ad-SYVN1 overexpressing SYVN1 (GenBank NM_172230.2) and vehicle control Ad-MCMV-MCS-HA (all by OBiO Technology, Shanghai, China) were introduced into hRMECs. The hRMECs (3 to 4 passages) were obtained from Cell Biologics and cultured in endothelial cell medium (ECM) supplemented with 5% fetal bovine serum (Gibco, USA), 100 U/mL of penicillin, and 100 U/mL of streptomycin at 37°C in an incubator (5% CO2). The cell was conducted at approximately 70% to 80% confluence using a 10 multiplicity of infection with Ad-SYVN1 or vehicle control. Moreover, 10 µM of MG-132 (MedChemExpress) and 1 µM of STAT3 activator Colivelin TFA (MedChemExpress) were used in combination with Ad-SYVN1. The 24 hours of post-transfection or infection, cells were exposed to a hypoxic gas environment with 1% O2, 94% N2, and 5% CO2 for 24 hours as a hypoxic model.

Experimental Animals and Intravitreal Injection

C57BL/6J mice were purchased from the Animal Laboratory of Shanghai Institute of Materia Medica. All procedures with animals were approved by the Institutional Animal Care and performed in accordance with the ARVO Statement for the Use of Animals in Ophthalmic and Vision Research.

The ROP model exposed P7 neonatal mice and pregnant female mice to a hyperoxia environment (75% ± 2% oxygen) for 5 days (P12) and then returned to room air for another 5 days (P17). At P12, the right eyes of OIR mice received an intravitreal injection of SYVN1 overexpression adenovirus (1×10^{11} pfu/mL, 1 µL), and the right eyes of the other groups received an intravitreal injection of the vehicle control Ad-MCMV-MCS-HA (1×10^{11} pfu/mL, 1 µL).

Tube Formation Assay

Fifty microliters of the Matrigel (Corning) were pre-coated into each well of a 96-well plate after thawing at 4°C. 2×10^4 hRMECs from each pretreatment per well in 50 µL of medium were seeded in 96-well plates after the matrix gel solidified. Images were photographed for each well using an inverted microscope at 10 × magnification (Olympus).

Co-Immunoprecipitation

Co-immunoprecipitation (Co-IP) was performed using a Pierce Co-IP kit (Invitrogen) according to the manufacturer's instructions, as described previously.[18] For immunoprecipitation of endogenous STAT3, anti-HA antibody (Invitrogen) was added to AminoLink Plus coupling resin or negative control resin. To assess ubiquitination, the protein samples were immunoprecipitated with an anti-FLAG antibody.

Western Blot Analysis

The protein levels in cultured hRMECs and mouse retinal tissues were lysed in RIPA lysis buffer (Cell Signaling Technology), measured using a BCA assay kit (Thermo Fisher Scientific). Western blot analyses were conducted and transferred to polyvinylidene fluoride membranes (Roche). Antibodies against SYVN1 (anti-HRD1), p-STAT3, STAT3, VEGFA, and TUBULIN were purchased from Cell Signaling Technology.

Reverse Transcription PCR

RNA was extracted from hRMECs using TRIzol reagent (Invitrogen). The PrimeScriptTM RT Reagent Kit (TaKaRa) was used for reverse transcription (RT). Quantitative real-time RT-PCR (qRT-PCR) was performed in triplicate on ViiA 7 (Applied Biosystems) using TB Green Premix Ex Taq (TaKaRa) with 20 µL reactions using specific primers (Supplementary Table S1). Relative mRNA levels were normalized to the levels of the β-actin using the $2^{-(\Delta\Delta Ct)}$ method.

Enzyme-Linked Immunosorbent Assay

The VEGF levels of 200 µL of HRMECs culture supernatants diluted with PBS were measured using a Human VEGF

Quantikine enzyme-linked immunosorbent assay (ELISA) kit (R&D Systems) according to the manufacturer's instructions. A 96-well microplate was coated with specific human VEGF monoclonal antibodies. The amount of cell VEGF was normalized to the total cell numbers.

Retinal Whole-Mounts

The enucleated eyes were placed in 4% paraformaldehyde (PFA; Sigma) for 2 hours. The retinas were dissected and processed under a microscope. We labeled the retinal vasculature with Isolectin B4-594 (Alexa Fluor 594-121413; Molecular Probes). The retinas were stained and mounted as described previously.[18] Merge images were taken in the Tile Scan module using a Leica TCS SP8 confocal microscope. Quantification of a vascularization (vaso-obliteration) was performed using Adobe Photoshop CS5 as previously described.[18] Neovascularization of retinal images was analyzed using ImageJ software.

Immunofluorescence Staining

Fixed retinal tissues were sectioned at 10-µm thickness through the optic disk. Sections were blocked with 5% BSA and 1% Triton X-100 in PBS for 1 hour. The slides were then incubated with SYVN1 antibody (1:200; Novus Biologicals), STAT3 antibody (1:500; Cell Signaling Technology), and CD31 antibody (1:100; Servicebio) and then individually incubated with secondary antibody (Alexa 488/594; Cell Signaling Technology; and Donkey anti-goat, 1:100; Servicebio) incubation for 1 hour. Slide nuclei were stained with 4′,6-diamidino-2-phenylindole DAPI (Invitrogen). After each incubation, the cells were washed three times. The fluorescence of the retinas was imaged using a confocal microscope.

Hematoxylin and Eosin Staining

Fixed retinal tissues were embedded in paraffin, sectioned at 10-µm thickness, and then stained with hematoxylin and eosin, as described previously.[18] RNV extent was measured by counting pre-retinal nuclei, which extended beyond the inner limiting membrane. The results are presented as the mean of neovascular nuclei per ocular cross-section.

Electroretinography

Retinal function was examined using the RETIport system (Roland consult) recorded from P17 mice by using scotopic full-field electroretinograms (ERGs). Mice were adapted overnight in the dark and anesthetized with 1% sodium pentobarbital. Pupils were dilated with 1% tropicamide. The body temperature was maintained at 37°C. The reference electrode was placed in the center of the scalp and the ground electrode was placed in the proximal portion of the tail skin. After the corneal surface was anesthetized, eye drops and contact-lens electrodes were applied directly to the corneal surface. All procedures were performed under dim red lighting. Mixed (rod and cone) responses were evoked by a luminance of 3.0 cd × s/m^2 generated through a Super color Ganzfeld stimulator (Q450 SC). The a-wave amplitude was defined as the negative wave just after light stimulation and the b-wave amplitude was measured from the a-wave to the peak of the b-wave. For each experimental condition, ERG analysis was performed on six mice.

Statistical Analysis

Numerical data are presented as the mean ± SD of at least three independent experiments. Two-tailed Student's *t*-test was used to analyze differences between experimental groups using GraphPad Prism software (version 8.0). The *P* values of < 0.05 were considered significant.

Results

Decreased SYVN1 Expression Observed in Hypoxia-Induced hRMECs and OIR Retina

To explore the role of SYVN1 in angiogenesis in vitro, we cultured hRMECs under hypoxic conditions (1% O2 and 5% CO2) for 24 hours. We observed significantly increased VEGF levels in hRMECs (Fig. 1A), accompanied by elevated protein expression levels of phospho-STAT3 (p-STAT3) and VEGFA (Fig. 1B), indicating that we successfully established the in vitro culture model. Endogenous SYVN1 protein abundance and transcriptional regulator mRNA levels decreased in hRMECs under hypoxic conditions, as expected (see Figs. 1B, 1C). However, hypoxia treatment did not alter the total STAT3 levels in hRMECs. Furthermore, we used the ROP mouse model to evaluate whether SYVN1 is involved in RNV. Analysis of retinal whole mounts demonstrated that OIR mice exhibited a large non-perfusion avascular area at P12 and a maximal extent of neovascular area at P17 (Fig. 1D). It is viable to use P17 OIR mice as a tool to investigate the pathogenesis of proliferative retinopathies as neovascularization spontaneously regresses at P30 (see Fig. 1D). As shown in Figure 1E, the endogenous expression of SYVN1 protein was markedly reduced in OIR retinal tissues compared with that in age-matched normoxia controls (NOIR group). In contrast, the hypoxic retina of mouse pups showed increased expression of p-STAT3, STAT3, and VEGFA compared with the normoxic retina of mice pups at P17 (see Fig. 1E), suggesting activation of STAT3 and VEGFA in hypoxia-induced RNV. We further evaluated its vascular distribution by localizing SYVN1 and CD31. Immunofluorescence (IF) staining revealed that SYVN1 was widely expressed in the retina, especially in the ganglion cell layer, inner nuclear layer, and inner segment layer. Significantly decreased SYVN1 in the pre-retinal neovascular vessels labeled by CD31 in magnified OIR retinal tissue images was observed, consistent with the results of Western blotting (Fig. 1F).

Taken together, these results demonstrate that SYVN1 is decreased under hypoxic conditions and is likely to be associated with neovascularization development in OIR.

Adenovirus-Mediated SYVN1 Overexpression Impedes Angiogenesis in the hRMECs

To further determine whether SYVN1 deficiency can initiate the pathogenesis of hypoxia-induced angiogenesis, we used hRMECs overexpression of SYVN1 via Ad-*SYVN1* transfection. Hypoxic stimulation promoted tube formation in hRMECs, whereas SYVN1 overexpression significantly inhibited this basic endothelial cell tube formation even at normal oxygen concentrations (Figs. 2A, 2B). ELISA further confirmed that SYVN1 overexpression significantly decreased the VEGF levels compared with vehicle treatment. Under hypoxia, this effect was more remarkable

Investigative Ophthalmology & Visual Science

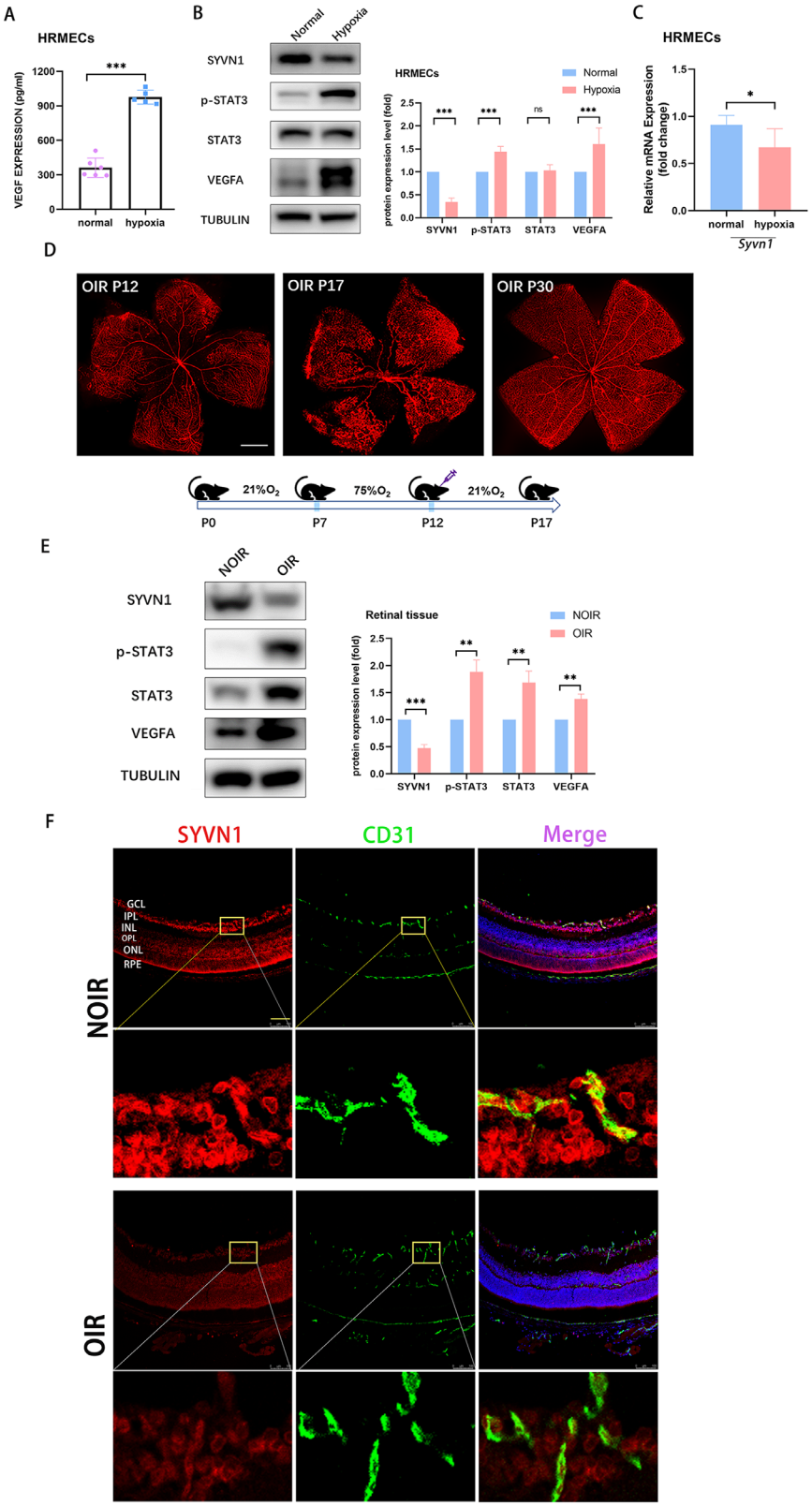

Figure 1. SYVN1 expression is decreased in hypoxia-induced hRMECs and OIR retina. (**A**) Secretion of VEGF in hRMECs culture supernates was analyzed using ELISA. Data represent mean ± SD (3 repeats). ***$P < 0.001$. (**B**) Western blot analysis and quantitation of SYVN1, p-STAT3, STAT3, and VEGFA protein levels in hRMECs between normoxic and hypoxia conditions by Western blot. Fold change in protein expression is expressed relative to the respective control. TUBULIN was used as internal control. Data represent mean ± SD (3 repeats). ***$P < 0.001$, ns, not significant. (**C**) The mRNA expression of *SYVN1* was determined by RT-PCR. Data are representative of three independent experiments. *$P < 0.05$. (**D**) Representative retinal whole mounts showing avascular area and NV among different phases in OIR mice (P12, P17, and P30). Scale bar = 1000 mm. (**E**) Western blot assay and quantitation of SYVN1, p-STAT3, STAT3, and VEGFA protein

Investigative Ophthalmology & Visual Science

levels in the retinas of NOIR and OIR mice. Fold change in protein expression is expressed relative to the respective control. TUBULIN was used as internal control. Data represent mean ± SD ($n = 6$). $^{**}P < 0.01$, $^{***}P < 0.001$; *t* test. (**F**) IF staining of CD31 (*green*) and SYVN1 (*red*) in retina sections of C57BL/6J mice in room air (NOIR mice) and induced C57BL/6J OIR mice. Each group contains eight mice. Scale bar = 100 µm.

(Fig. 2C). These results suggested that infection of Ad-*SYVN1* suppresses hypoxia-induced angiogenesis in hRMECs.

Next, we verified the possible connection between STAT3 and SYVN1. The expressions of endogenous STAT3, p-STAT3, and VEGFA were significantly decreased after SYVN1 overexpression in hRMECs under both normoxia and hypoxia. This suggests that the inhibitory effect of SYVN1 on tube formation in hRMECs may be related to STAT3/VEGFA activity (Fig. 2D). As shown in Figure 2E, the mRNA level of STAT3 did not significantly change after SYVN1 overexpression under both environments, indicating that SYVN1 decreases STAT3 expression level at the post-translational level.

Collectively, the hypoxia-mediated reduction of SYVN1 contributes more to the abnormal activation of STAT3/VEGF signaling cascades and subsequent neovascularization in hRMECs (Fig. 3A).

SYVN1 Inhibits STAT3 Activity by Ubiquitin-Mediated Protein Degradation

As an E3 ligase, SYVN1 may be involved in regulating the stability of STAT3 through ubiquitin-mediated protein degradation. Here, first, we introduced a comprehensive database, UbiBrowser, to predict ubiquitin ligase/ deubiquitinase-substrate interactions. SYVN1 is shown as a predicted candidate (see Fig. 3A). Next, we confirmed the predicted interaction between the E3 ligase (SYVN1) and the substrate (STAT3). Cell lysates from hRMECs under hypoxic conditions with different dosages of Ad-*SYVN1*-HA were measured. We observed STAT3 expression progressively decreased in a dose-dependent manner (Fig. 3B), compared with the Ad-ctrl-HA control group, indicating a potential negative correlation between SYVN1 and STAT3. As mentioned in Figure 2E, this decrease was due to protein degradation at the post-translational level. Then, we used chemical inhibitors. Downregulation of STAT3 protein levels and increased VEGFA expression were significantly rescued under hypoxic conditions by treating with 20 µM of MG-132, a reversible proteasome inhibitor rather than 100 µM of leupeptin, a lysosomal enzyme inhibitor (Fig. 3C). Next, hRMECs were co-transfected with HA-tagged SYVN1 and MG-132. The Co-IP assay identified a physical interaction between SYVN1 E3 ubiquitin ligase and STAT3, whereas the control yielded no STAT3 signal. The treatment of MG132 obviously increased STAT3 signal when compared with the control (Fig. 3D). To shed light on their cellular localization where SYVN1 interacts with STAT3 in cells, a double-labeling IF technique was used. Although most of the STAT3 protein was located in the nucleus, SYVN1 in cells could be clearly observed in the cytoplasm and nucleoplasm, co-localizing with STAT3 (Fig. 3E). Next, we explored whether STAT3 could be modified by ubiquitination. After co-transducing hRMECs with Ad-*SYVN1* and ubiquitin-FLAG, FLAG-tagged proteins were immunoprecipitated, and immunoblotting was performed using SYVN1 or STAT3. Co-IP results validated the elevated ubiquitination level of STAT3 pretreated for 4 hours with MG-132 under normoxia compared with the vehicle control (Fig. 3F). Accordingly, these data demonstrate a critical and efficiently regulated process by which SYVN1 interacts with STAT3 and promotes its ubiquitylation and degradation.

STAT3 Activator Suppresses Protective Effect of SYVN1 Against Angiogenesis

To examine whether the protective effect of SYVN1 against angiogenesis in hRMECs was dependent on the STAT3/VEGF axis, we transfected Ad-*SYVN1* into cells preconditioned with colivelin TFA, a potent activator of STAT3, for 4 hours. Western blotting and ELISA revealed that the decreased STAT3/VEGF activity was rescued after colivelin TFA administration compared with Ad-*SYVN1* alone whether underwent hypoxia stimulating or not (Figs. 4A, 4B). TFA significantly increased tube formation in *SYVN1*-treated hRMECs, while more pronounced effects in hypoxia-treated hRMECs were observed. This indicates that the SYVN1 inhibitory effect on hRMECs' basal activity function in normoxia and its' protection against angiogenesis under hypoxia is dependent on the STAT3 activity (Figs. 4C, 4D). These results suggest that SYVN1 inhibits neovascularization in a STAT3-dependent manner by promoting STAT3 ubiquitylation and degradation.

SYVN1 Gene Manipulation Further Inhibits Avascular and Neovascularization Retinal Through STAT3/VEGF Signaling Pathway in the ROP Mouse Model

To verify whether *SYVN1* is a key regulator of the STAT3/VEGF axis and has a significant impact on angiogenesis in vivo, Ad-*SYVN1* was injected into the vitreous cavity on 12-day-old control mice and P12 OIR mice. Unsurprisingly, the levels of p-STAT3, STAT3, and VEGFA were suppressed in the retinal tissues of P17 control mice and OIR mice injected with Ad-*SYVN1* (Fig. 5A). Co-labeling of STAT3 with SYVN1 was also observed in the sections from the NOIR and OIR model (Fig. 5B), with stronger fluorescence intensity after SYVN1 overexpression, indicating that SYVN1 suppresses angiogenesis by blocking the STAT3/VEGF signaling pathway.

Furthermore, we observed the inhibitory effect of SYVN1 on pathological vessel proliferation. As shown in Fig. 5C, the regular vascular development was not affected by SYVN1 under normoxia, whereas the nonperfusion area and RNV were obvious under hypoxia. Injection of Ad-*SYVN1* in OIR mice resulted in a less avascular area in the central retina at P17 and was also effective in protecting the retina from pathological vessel proliferation corresponding to robust RNV changes (the vessel tuft area) at P17 compared with control mice (see Fig. 5C). These data suggest that the decrease of endogenous SYVN1 during the proliferative phase of retinopathy results in increased RNV. In addition, hematoxylin and eosin (H&E) staining demonstrated that SYVN1 overexpression maintained the normal retinal layer structure and significantly inhibited the increase in

Investigative Ophthalmology & Visual Science

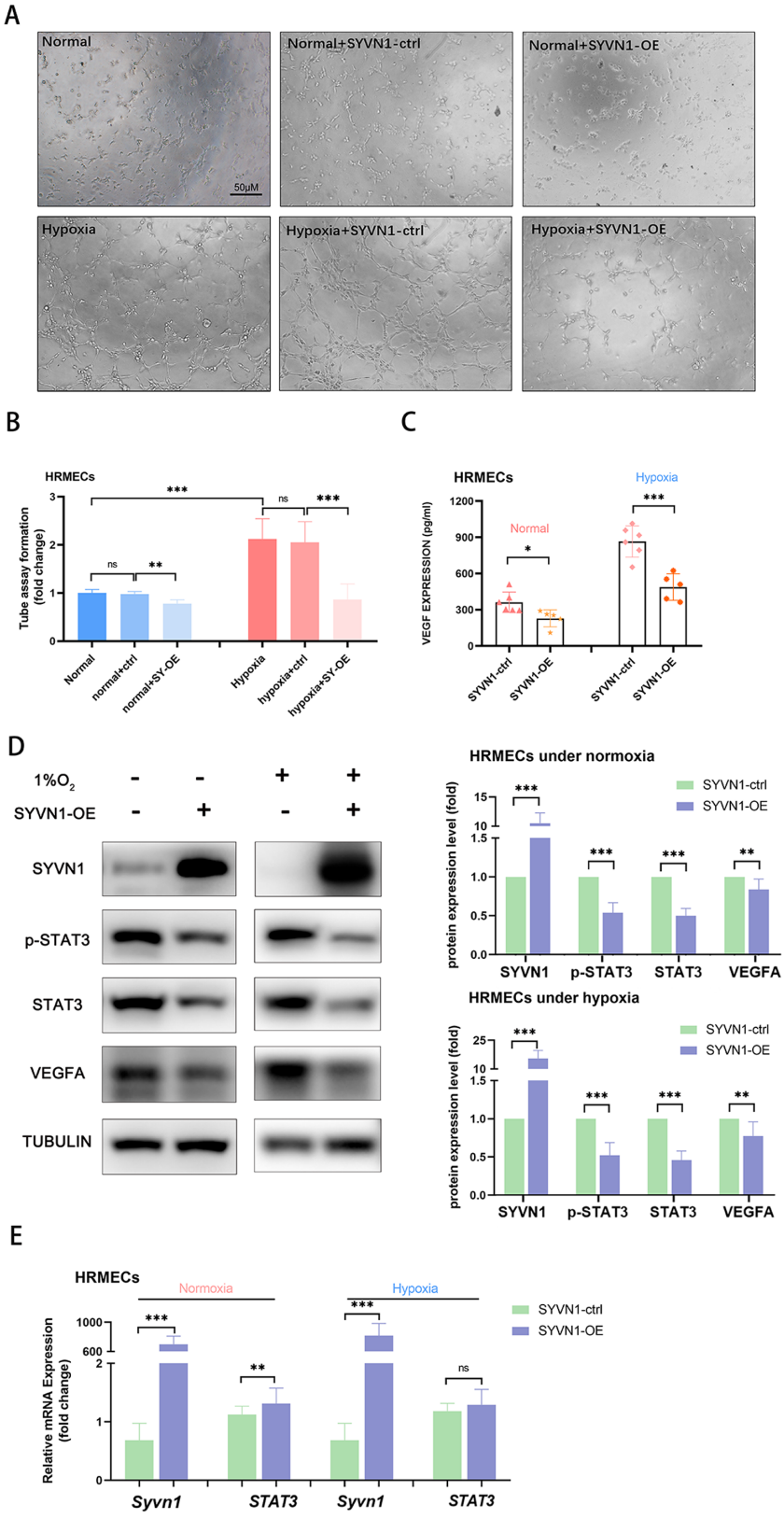

Figure 2. SYVN1 regulates angiogenesis in hypoxia-induced hRMECs. (**A**) Representative images of Tube formation assay. (**B**) Average length of tube formation for each field was statistically analyzed using the tool "Angiogenesis Analyzer" in ImageJ software. Data represent mean ± SD (3 repeats). $^{**}P < 0.01$, $^{***}P < 0.001$; *t* test. Scale bar = 50 μm. (**C**) Secretion of VEGF in hRMECs culture supernates was analyzed using ELISA. Data represent mean ± SD (3 repeats). $^{***}P < 0.001$; *t* test. (**D**) Western blot analysis and quantitation of SYVN1, p-STAT3, STAT3, and VEGFA protein levels in hRMECs with *Ad-SYVN1*transfection under normoxia or hypoxia as indicated. TUBULIN was used as internal control. Data represent mean ± SD (3 repeats). $^{**}P < 0.01$, $^{***}P < 0.001$; *t* test. (**E**) The mRNA expression of *SYVN1* and *Stat3* was determined by qRT-PCR. Data are representative of three independent experiments. $^{***}P < 0.001$; ns, not significant.

Investigative Ophthalmology & Visual Science

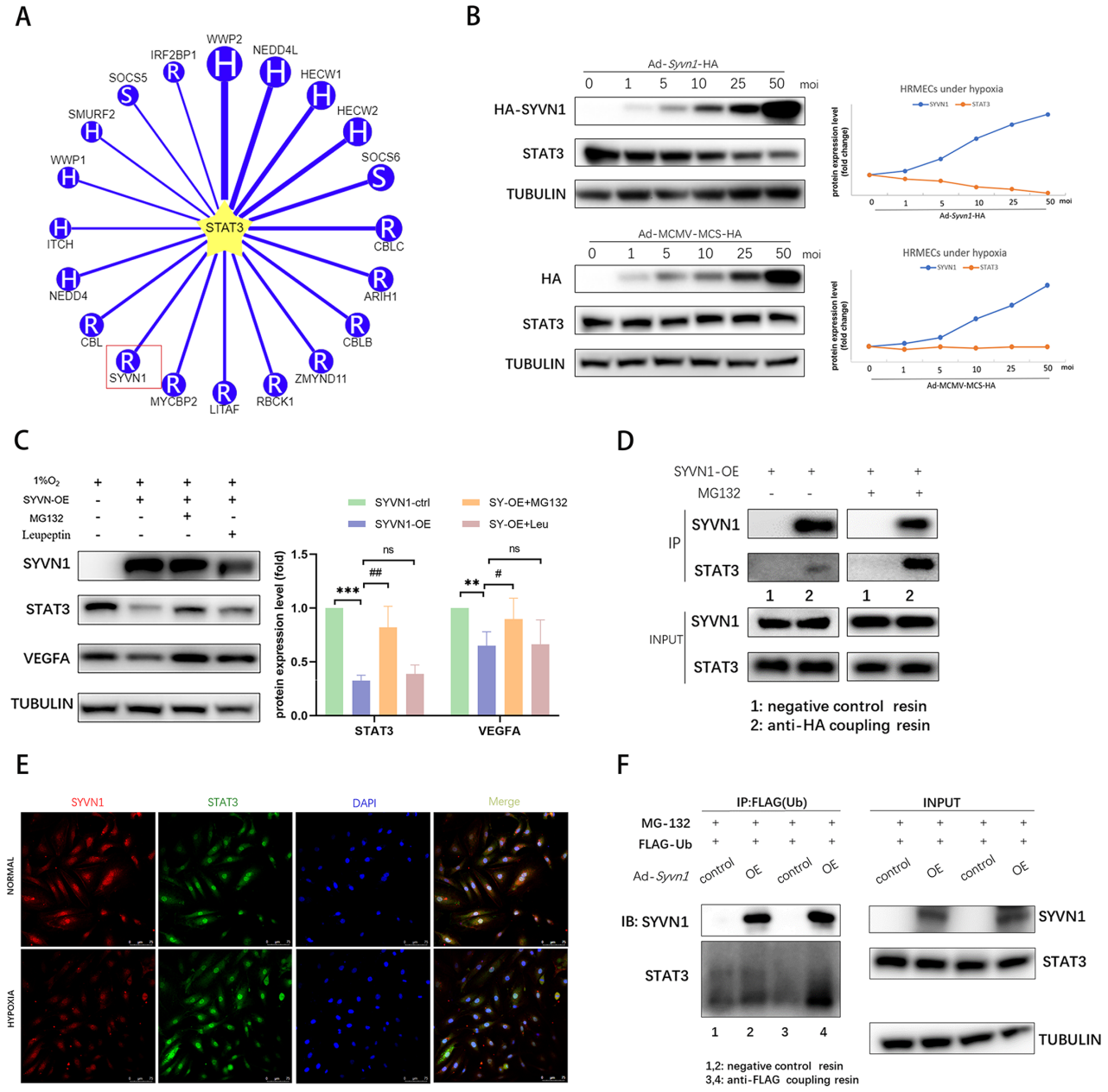

Figure 3. SYVN1 interacts with STAT3 through its ubiquitination activity. (**A**) Prediction results of the top 20 predicted E3 ligases for STAT3 substrates using the UbiBrowser database (http://ubibrowser.ncpsb.org.cn). (**B**) The different concentration gradients of Ad-*SYVN1*-HA or Ad-ctrl-HA were transfection to the hRMECs under hypoxia. The protein level of STAT3 protein from cell lysates with the multiplicity of infection at 0, 1, 5, 10, 25, and 50 was detected by Western blotting. (**C**) Comparison of SYVN1, STAT3, and VEGFA levels in mRMECs with different treatment by Western blot. TUBULIN was used as a loading control. The *right panels* show densitometric analysis of Western blots. Fold change in protein expression is expressed relative to the respective control. Data are representative of three independent experiments. $^{\#}P < 0.05$; $^{**}P < 0.01$; $^{\#\#}P < 0.01$; $^{***}P < 0.001$; ns, not significant; *t* test. (**D**) The hRMECs were transfected with HA-*SYVN1*-OE, with or without MG132 pretreatment (a proteasome inhibitor). The anti-HA antibody was used in immunoprecipitation (IP) combine with AminoLink Plus coupling resin or negative control resin, the SYVN1 and STAT3 antibody was used in immunoblotting (IB). (**E**) The protein levels and distribution of SYVN1 (*red*) and STAT3 (*green*) in hRMECs with different treatment were detected through immunofluorescence assay. DAPI indicated nucleus. Scale bar = 75 µm. (**F**) The hRMECs were transfected with HA-*SYVN1*-OE and FLAG-Ub followed by the treatment of MG132. The anti-FLAG antibody was used in immunoprecipitation (IP) combine with AminoLink Plus coupling resin or negative control resin, the SYVN1 and SYAY3 antibody was used in immunoblotting (IB).

pre-retinal neovascular vessels in the OIR group, as indicated by the number of neovascular nuclei (Fig. 5D). Because reports have demonstrated that the visual function of OIR mice is damaged, we determined the effect of SYVN1 on ocular functional characteristics to light stimulation. OIR mice displayed significantly reduced scotopic a- and b-waves, as assessed by ERG functional analysis. Intravitreal administrations of Ad-SYVN1 did not influence retinal responses in room air mice or OIR mice (Fig. 5E).

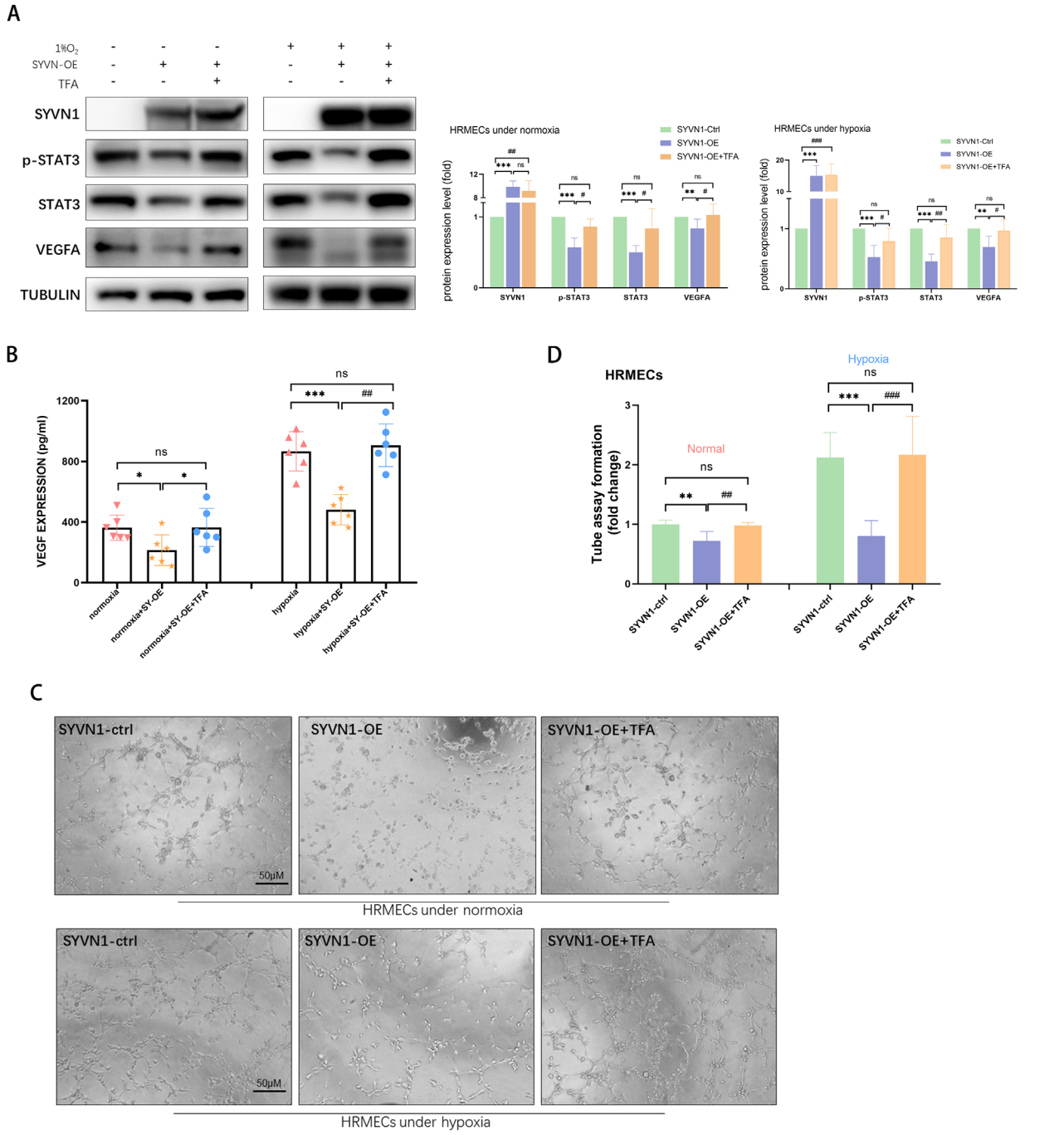

Figure 4. Hypoxia-mediated SYVN1 reduction promotes tube formation in mRMECs through elevating STAT3 activity. (**A**) Western blot analysis of effects of *SYVN1*-OE or in combination with STAT3 inhibitor colivelin TFA on STAT3/VEGFA pathway under normoxia and hypoxia. Fold change in protein expression is expressed relative to the respective control. Data are representative of three independent experiments. $^{*}P < 0.05$; $^{\#}P < 0.05$; $^{**}P < 0.01$, $^{\#\#}P < 0.01$; $^{***}P < 0.001$;, $^{\#\#\#}P < 0.001$; ns, not signification; *t* test. (**B**) Secretion of VEGF in hRMECs culture supernates was analyzed using ELISA. Data represent mean ± SD (3 repeats). $^{\#\#}P < 0.01$; $^{***}P < 0.001$; ns, not signification; *t* test. (**C**) Representative images of Tube formation assay. (**D**) Average length of tube formation for each field was statistically analyzed using the tool "Angiogenesis Analyzer" in ImageJ software. Data represent mean ± SD (3 repeats). $^{\#\#\#}P < 0.001$; $^{***}P < 0.001$; ns, not signification; *t* test. Scale bar = 50 μm.

Investigative Ophthalmology & Visual Science

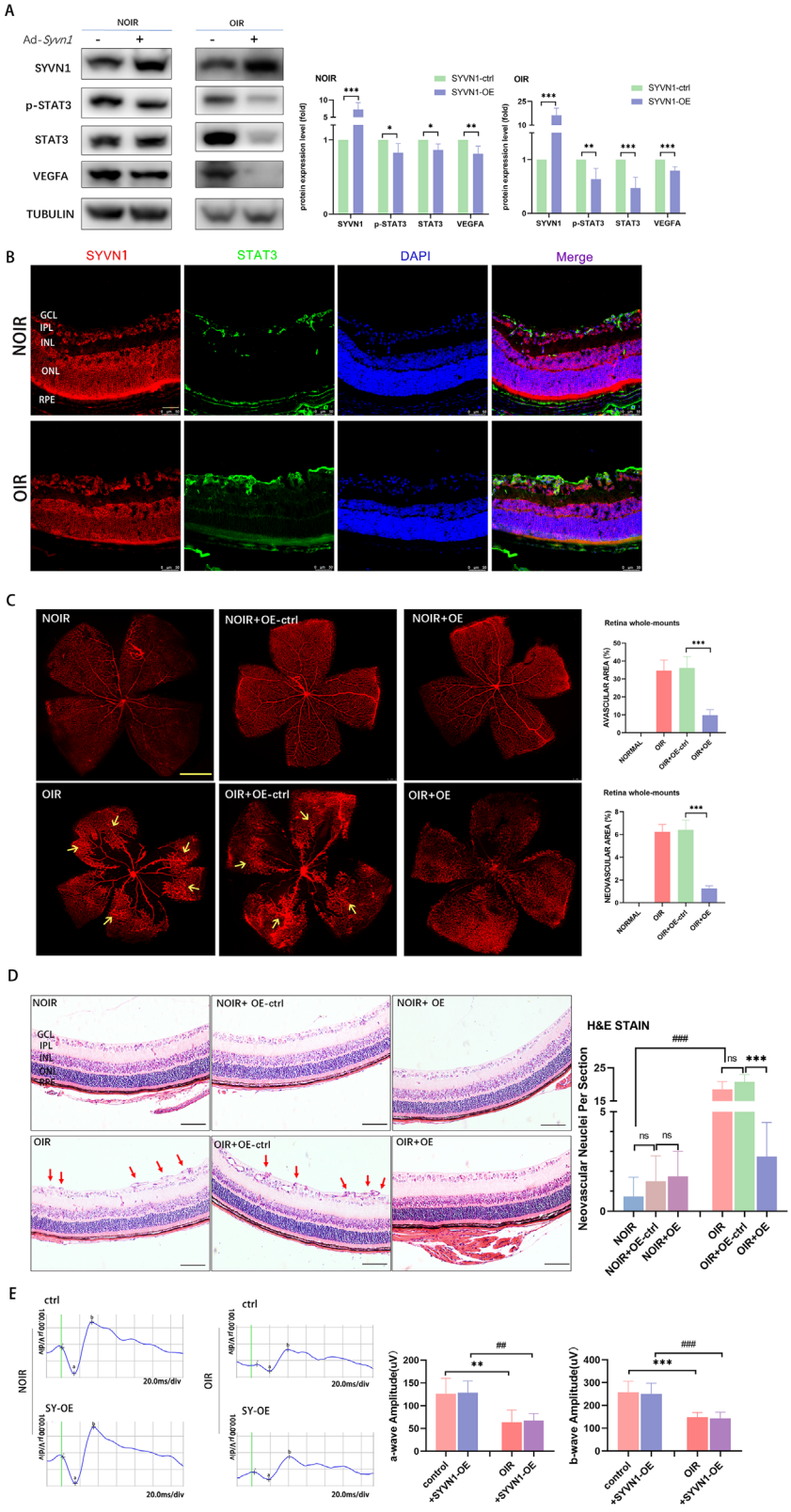

Figure 5. SYVN1 overexpression inhibits neovascularization in OIR mice. (**A**) Ad-*SYVN1* overexpression intravitreal injection inhibits STAT3 and VEGFA levels in retinal tissue by Western blot. The *right panel* shows densitometric analysis of Western blots. Fold change in protein expression is expressed relative to the respective control ($n = 6$). $^{**}P < 0.01$; $^{***}P < 0.001$; *t* test. (**B**) Co-labeling of STAT3 (*green*) with SYVN1 (*red*) in sections from the normal (NOIR) and OIR model was detected through immunofluorescence assay. DAPI indicated nucleus. Scale bar = 50 µm. (**C**) Retinal vascular development in normal and OIR mice (P17). Representative retinal whole mounts showing avascular area and NV after intravitreal injection of *SYVN1*-OE and vehicle control as indicated. retinal whole-mount with the total avascular

area *highlighted in yellow*. Neovascular tufts are indicated by arrows. Data represent mean ± SD ($n = 10$). ns, not significant; ***$P < 0.001$; *t* test. Scale bar = 1000 mm. (**D**) H&E staining of retinas. Neovascular nuclei are indicated by red arrows. The number of nuclei per retinal area was quantitated. Data represent mean ± SD ($n = 10$). ***$P < 0.001$; *t* test. Scale bar = 50 µm. (**E**) Representative ERG waveforms in control and in OIR mice, untreated or treated with Ad-*SYVN1* recorded at light intensity of 3 log cd-s m^{-2}, represent, respectively, a-wave amplitudes (means ± SE) and b-wave amplitudes (means ± SE) in control and in OIR mice untreated or treated with Ad-*SYVN1*. Values represent means ± SE ($n = 6$). **$P < 0.01$; ***$P < 0.001$; *t* test.

Discussion

The pathological angiogenesis of ROP is extraordinarily complicated. The safety issue of anti-VEGF therapy is always under concern.[33,34] Thus, there is an urgent need to screen out an effective therapeutic target. Previous studies have reported that ER stress markers are involved in vascular impairment in DR.[35,36] The effects of SYVN1 are related to chronic inflammation and ER stress in the retinas of diabetic mice.[31] However, whether SYVN1 is involved in neovascularization and the mechanism of this process has not yet been fully clarified in ROP. Therefore, in this study, we focused on the role of SYVN1 in neovascularization and its possible mechanism for ROP.

In our study, SYVN1 expression was downregulated in vitro in hRMECs cultured under hypoxia and in vivo oxygen-induced mouse retinal tissue, revealing that SYVN1 is a promising therapeutic candidate for RNV-associated disease. The protective effects of SYVN1 in OIR mice are associated with the inhibition of the STAT3/VEGF axis via the ubiquitin-mediated protein degradation pathway. Many studies have reported that the E3 ligase of SYVN1 is responsible for the ubiquitination and degradation of downstream proteins, such as P53, sirtuin 2, and insulin like growth factor I receptor, which are associated with some key biological processes.[37–39] In agreement with these conclusions, we also found that SYVN1 regulates STAT3/VEGF activity through its E3 ubiquitin-protein ligase activity. What's more, the ubiquitin-proteasome system regulates cell proliferation, differentiation, apoptosis, and other biological processes, which have an important and profound influence on cell fate.[40] Data from the Human Protein Atlas showed that SYVN1 was detected in the nucleoplasm, ER, and plasma membrane, which is consistent with the IF results illustrated in Figure 3. As shown in Figure 3E, SYVN1 in cells could be clearly observed in the cytoplasm and nucleoplasm, co-localizing with STAT3. Hypoxic stimulation reduced endogenous expression of SYVN1, while the ubiquitination and degradation of STAT3 protein noticeably decreased in cells. The reduced abundance of SYVN1 substantially weakened their interaction, resulting in a more concentrated and nuclear localization of STAT3, enabling its function as a nuclear transcription factor. STAT3 transcriptional activity was exerted in the nucleus, suggesting that the interaction between SYVN1 and STAT3 is not regulated by its transcriptional activity. The effect of SYVN1 overexpression on STAT3 activity was reversed by STAT3 activation. We also confirmed that SYVN1 can negatively regulate angiogenesis through the downstream effects of ubiquitination of STAT3, such as the regulation of the angiogenic gene VEGF. These results indicate a novel upstream target for the therapeutic prevention of pathophysiological RNV.

For the ROP treatment, reducing IVNV and resuming physiological vascularity are both important.[41,42] This study shows that the avascular and neovascular areas are smaller in the Ad-*SYVN1* treatment group than in the control group, indicating that SYVN1 not only inhibits the pathological neovasculature but also promotes physiological vessel regrowth. Simmons et al.[23] reported that STAT3 knockdown efficiently inhibited VEGF-induced retinopathy without delaying physiological retinal vascular development, which agrees with our findings. The underlying mechanism of SYVN1 promoting central retinal vasculature restoration is unclear. As SYVN1 is a core member of the ER-transmembrane E3 ligase complex involved in ER stress and is activated in vascular endothelial cells in pathogenic retinal diseases,[43,44] we postulate that SYVN1 targets specific substrates (STAT3) and promotes unfolded protein degradation by mediating the effects of ERAD in vascular endothelial cells in pathogenic retinal diseases to maintain cell homeostasis, what's more leads to the protection of physiological vascular density in ROP progression.

However, the anti-angiogenic effect of SYVN1 in OIR retinas did not seem to rescue the visual function, as indicated by the electroretinographic responses in vehicle- and SYVN1-treated OIR retinas. We speculate that improved ERG response may be detectable at a later time point after Ad-SYVN1 treatment, although there is also evidence indicating that effective treatment in reducing physiological and pathological angiogenesis may not prevent retinal dysfunction.[45] The ERG study result, at least in part, proves that SYVN1 injected intravitreally does not harm the visual function. Coupled with the fact that ROP is also a neurodegenerative disease,[46] the mechanisms underlying retinal neuronal damage in oxygen-induced retinopathy need further exploration.

In summary, our results provide important insights into new strategies for the prevention and treatment of ROP. Intravitreal injection of SYVN1 showed significant anti-neovascularization effects in OIR mouse and retinal microvascular endothelial cell models. The role of SYVN1 in promoting central retinal vasculature restoration lays the foundation for further research on the underlying mechanism for better combating RNV in ROP.

Acknowledgments

The authors thank all members of the Chinese Academy of Sciences Shanghai Institute of Materia Medica and Shanghai Key Laboratory of Ocular Fundus Diseases for their expertise and technical assistance.

Supported by the Medical Engineering Intersecting Research Fund of Shanghai Jiao Tong University (No. YG2019QNA59), the National Key R&D Program of China (2016YFC0904800, 2019YFC0840607), the National Science and Technology Major Project of China (2017ZX09304010), and Shanghai Key Clinical Specialty.

Disclosure: **S. Chen**, None; **J. Zhang**, None; **D. Sun**, None; **Y. Wu**, None; **J. Fang**, None; **X. Wan**, None; **S. Li**, None; **S. Zhang**, None; **Q. Gu**, None; **Q. Shao**, None; **J. Dong**, None; **X. Xu**, None; **F. Wei**, None; **Q. Sun**, None

References

1. Hellström A, Smith LE, Dammann O. Retinopathy of prematurity. *Lancet*. 2013;382(9902):1445–1457.
2. Lawn JE, Davidge R, Paul VK, et al. Born too soon: care for the preterm baby. *Reprod Health*. 2013;10(Suppl 1):S5.
3. Bancalari A, Schade R. Update in the treatment of retinopathy of prematurity. *Am J Perinatol*. 2022;39(1):22–30.
4. Blencowe H, Lawn JE, Vazquez T, Fielder A, Gilbert C. Preterm-associated visual impairment and estimates of retinopathy of prematurity at regional and global levels for 2010. *Pediatr Res*. 2013;74(Suppl 1):35–49.
5. Gergely K, Gerinec A. Retinopathy of prematurity–epidemics, incidence, prevalence, blindness. *Bratisl Lek Listy*. 2010;111(9):514–517.
6. Zhang RH, Liu YM, Dong L, et al. Prevalence, years lived with disability, and time trends for 16 causes of blindness and vision impairment: findings highlight retinopathy of prematurity. *Front Pediatr*. 2022;10:735335.
7. Chan-Ling T, Gole GA, Quinn GE, Adamson SJ, Darlow BA. Pathophysiology, screening and treatment of ROP: a multi-disciplinary perspective. *Prog Retin Eye Res*. 2018;62:77–119.
8. Pétursdóttir D, Holmström G, Larsson E. Visual function is reduced in young adults formerly born prematurely: a population-based study. *Br J Ophthalmol*. 2020;104(4):541–546.
9. Darlow BA, Elder MJ, Kimber B, Martin J, Horwood LJ. Vision in former very low birthweight young adults with and without retinopathy of prematurity compared with term born controls: the NZ 1986 VLBW follow-up study. *Br J Ophthalmol*. 2018;102(8):1041–1046.
10. Lepore D, Quinn GE, Molle F, et al. Intravitreal bevacizumab versus laser treatment in type 1 retinopathy of prematurity: report on fluorescein angiographic findings. *Ophthalmology*. 2014;121(11):2212–2219.
11. Hartnett ME, Penn JS. Mechanisms and management of retinopathy of prematurity. *N Engl J Med*. 2012;367(26):2515–2526.
12. Tsai AS, Chou HD, Ling XC, et al. Assessment and management of retinopathy of prematurity in the era of anti-vascular endothelial growth factor (VEGF). *Prog Retin Eye Res*. 2022;88:101018.
13. Wu WC, Lien R, Liao PJ, et al. Serum levels of vascular endothelial growth factor and related factors after intravitreous bevacizumab injection for retinopathy of prematurity. *JAMA Ophthalmol*. 2015;133(4):391–397.
14. Casini G, Dal Monte M, Fornaciari I, Filippi L, Bagnoli P. The β-adrenergic system as a possible new target for pharmacologic treatment of neovascular retinal diseases. *Prog Retin Eye Res*. 2014;42:103–129.
15. Morin J, Luu TM, Superstein R, et al. Neurodevelopmental outcomes following bevacizumab injections for retinopathy of prematurity. *Pediatrics*. 2016;137(4):e20153218.
16. Xi L. Combination of pigment epithelium derived factor with anti-vascular endothelial growth factor therapy protects the neuroretina from ischemic damage. *Biomed Pharmacother*. 2022;151:113113.
17. Wang J, Wang X, Gao Y, et al. Stress signal regulation by Na/K-ATPase as a new approach to promote physiological revascularization in a mouse model of ischemic retinopathy. *Invest Ophthalmol Vis Sci*. 2020;61(14):9.
18. Chen S, Sun Q, Sun D, et al. C-CBL is required for inhibition of angiogenesis through modulating JAK2/STAT3 activity in ROP development. *Biomed Pharmacother*. 2020;132:110856.
19. Levy DE, Darnell JE Stats: transcriptional control and biological impact. *Nat Rev Mol Cell Biol*. 2002;3(9):651–662.
20. Mohan CD, Rangappa S, Preetham HD, et al. Targeting STAT3 signaling pathway in cancer by agents derived from Mother Nature. *Semin Cancer Biol*. 2022;80:157–182.
21. Wang H, Byfield G, Jiang Y, Smith GW, McCloskey M, Hartnett ME. VEGF-mediated STAT3 activation inhibits retinal vascularization by down-regulating local erythropoietin expression. *Am J Pathol*. 2012;180(3):1243–1253.
22. Simmons AB, Bretz CA, Wang H, et al. Gene therapy knockdown of VEGFR2 in retinal endothelial cells to treat retinopathy. *Angiogenesis*. 2018;21(4):751–764.
23. Xu Y, Melo-Cardenas J, Zhang Y, et al. The E3 ligase Hrd1 stabilizes Tregs by antagonizing inflammatory cytokine-induced ER stress response. *JCI Insight*. 2019;4(5):e121887.
24. Lu Y, Qiu Y, Chen P, et al. ER-localized Hrd1 ubiquitinates and inactivates Usp15 to promote TLR4-induced inflammation during bacterial infection. *Nat Microbiol*. 2019;4(12):2331–2346.
25. Gao B, Lee SM, Chen A, et al. Synoviolin promotes IRE1 ubiquitination and degradation in synovial fibroblasts from mice with collagen-induced arthritis. *EMBO Rep*. 2008;9(5):480–485.
26. McLaughlin T, Medina A, Perkins J, Yera M, Wang JJ, Zhang SX. Cellular stress signaling and the unfolded protein response in retinal degeneration: mechanisms and therapeutic implications. *Mol Neurodegener*. 2022;17(1):25.
27. Zhang SX, Ma JH, Bhatta M, Fliesler SJ, Wang JJ. The unfolded protein response in retinal vascular diseases: implications and therapeutic potential beyond protein folding. *Prog Retin Eye Res*. 2015;45:111–131.
28. Gorbatyuk MS, Starr CR, Gorbatyuk OS. Endoplasmic reticulum stress: new insights into the pathogenesis and treatment of retinal degenerative diseases. *Prog Retin Eye Res*. 2020;79:100860.
29. Christianson JC, Olzmann JA, Shaler TA, et al. Defining human ERAD networks through an integrative mapping strategy. *Nat Cell Biol*. 2011;14(1):93–105.
30. Shruthi K, Reddy SS, Reddy GB. Ubiquitin-proteasome system and ER stress in the retina of diabetic rats. *Arch Biochem Biophys*. 2017;627:10–20.
31. Yang S, He H, Ma QS, et al. Experimental study of the protective effects of SYVN1 against diabetic retinopathy. *Sci Rep*. 2015;5:14036.
32. Zhang J, Chen C, Wu L, et al. Synoviolin inhibits the inflammatory cytokine secretion of Müller cells by reducing NLRP3. *J Mol Endocrinol*. 2022;68(2):125–136.
33. Lepore D, Quinn GE, Molle F, et al. Follow-up to age 4 years of treatment of type 1 retinopathy of prematurity intravitreal bevacizumab injection versus laser: fluorescein angiographic findings. *Ophthalmology*. 2018;125(2):218–226.
34. Stahl A, Lepore D, Fielder A, et al. Ranibizumab versus laser therapy for the treatment of very low birthweight infants with retinopathy of prematurity (RAINBOW): an open-label randomised controlled trial. *Lancet*. 2019;394(10208):1551–1559.
35. Adachi T, Yasuda H, Nakamura S, et al. Endoplasmic reticulum stress induces retinal endothelial permeability of extracellular-superoxide dismutase. *Free Radic Res*. 2011;45(9):1083–1092.
36. Yang L, Wu L, Wang D, et al. Role of endoplasmic reticulum stress in the loss of retinal ganglion cells in diabetic retinopathy. *Neural Regen Res*. 2013;8(33):3148–3158.
37. Ji F, Zhou M, Sun Z, et al. Integrative proteomics reveals the role of E3 ubiquitin ligase SYVN1 in hepatocellular carcinoma metastasis. *Cancer Commun (Lond)*. 2021;41(10):1007–1023.
38. Huang Y, Sun Y, Cao Y, et al. HRD1 prevents apoptosis in renal tubular epithelial cells by mediating eIF2α

ubiquitylation and degradation. *Cell Death Dis*. 2017;8(12):3202.

39. Liu L, Yu L, Zeng C, et al. E3 ubiquitin ligase HRD1 promotes lung tumorigenesis by promoting sirtuin 2 ubiquitination and degradation. *Mol Cell Biol*. 2020;40(7):e00257–19.
40. Hoeller D, Hecker CM, Dikic I. Ubiquitin and ubiquitin-like proteins in cancer pathogenesis. *Nat Rev Cancer*. 2006;6(10):776–788.
41. Rivera JC, Dabouz R, Noueihed B, Omri S, Tahiri H, Chemtob S. Ischemic retinopathies: oxidative stress and inflammation. *Oxid Med Cell Longev*. 2017;2017:3940241.
42. Connor KM, Krah NM, Dennison RJ, et al. Quantification of oxygen-induced retinopathy in the mouse: a model of vessel loss, vessel regrowth and pathological angiogenesis. *Nat Protoc*. 2009;4(11):1565–1573.
43. Ruggiano A, Foresti O, Carvalho P. Quality control: ER-associated degradation: protein quality control and beyond. *J Cell Biol*. 2014;204(6):869–879.
44. Qi L, Tsai B, Arvan P. New Insights into the physiological role of endoplasmic reticulum-associated degradation. *Trends Cell Biol*. 2017;27(6):430–440.
45. Hatzopoulos KM, Vessey KA, Wilkinson-Berka JL, Fletcher EL. The vasoneuronal effects of AT1 receptor blockade in a rat model of retinopathy of prematurity. *Invest Ophthalmol Vis Sci*. 2014;55(6):3957–3970.
46. Hansen RM, Moskowitz A, Akula JD, Fulton AB. The neural retina in retinopathy of prematurity. *Prog Retin Eye Res*. 2017;56:32–57.

Investigative Ophthalmology & Visual Science